

WALKING QUADRUPED WITH SUPPORT/STEERING WHEELS

Ashwin Mudigonda

Dept. of Electrical Engineering,
Ohio University,
329, Stocker Center,
Athens, OH-45701, USA
m_ashwin_81@yahoo.com

Robert L. Williams II

Dept. of Mechanical Engineering,
Ohio University
259, Stocker Center
Athens, OH-45701, USA
bobw@bobcat.ent.ohiou.edu

Abstract- This paper presents a new design for a walking quadruped. It incorporates a support/steering axle with two wheels always in contact with the ground to ensure the quadruped can stably lift two legs during gaits. Abilities include following complex trajectories. Kinematics, forward-pose gaits, and simulation examples are presented in this paper.

bound, and do several transitions between gaits. It was found that principles for one-legged hopping could be generalized to four-legged running, with the addition of a low-level leg coordination mechanism. The Quadruped generated different types of gaits like trotting (diagonal legs as pairs), pacing (lateral pairs), and bounding (front pair and rear pair).

I. INTRODUCTION

Walking and running machines are classified into two categories based on the stability of their motion: passively stable and dynamically stable. For a passively stable system, the vertical projection of the center of mass always remains within the closed region formed by the contact points of the feet on the ground. This region is called the support polygon. They typically have four or six legs but may be bipeds with large foot surface area. In contrast, dynamically stable systems utilize dynamic forces and feedback to maintain balance. Dynamically stable machines have been built with one, two, and four legs. Because dynamically stable systems are more difficult to design, control and analyze, the early legged robots were mostly statically stable machines.

Robert McGhee of Ohio State University built a Hexapod in 1977 by using electric drill motors (Bucket 1977; McGhee 1983). A second hexapod from OSU, the Adaptive Suspension Vehicle, was a three-ton vehicle with a human driver but automatic positioning of the legs (Song and Waldron 1989). Many designs have been proposed to simplify both mechanical considerations and the load on the processor for maintaining balance. For example, Shigeo Hirose's 1980 PV II quadruped incorporated a pantograph leg mechanism that allowed actuators independently to control each degree of freedom in Cartesian space, considerably simplifying the kinematics pose equations (Hirose and Umetani 1980). The Ambler, a thirty-foot-tall, hexapod planetary explorer built at Carnegie Mellon University, used an orthogonal leg design to simplify the kinematics equations (Simmons et al. 1992). Another robot built at CMU, Dante, used sets of legs mounted on sliding frames. In 1994, Dante II successfully descended into an active volcano in Alaska and analyzed high temperature gases

The Quadruped, built by MIT during 1984-1987 was used to explore running on four legs. It was programmed to trot, pace,

Quadrupeds designed to date either have to be tethered from above or need to have a low clearance. Dynamic systems need to have bulky control actuators and also have to carry along on-board microcontrollers to control them. This leaves little space for payload. A wheeled mechanism provides fast and efficient locomotion on flat terrain, while legged locomotion is capable of adapting to a hostile terrain. Marrying wheels and legs, called Whlegs (Quinn, R. D. Nelson et al., 2001) is a new concept under development. "Walk'n Roll", built by the Mechanical Engineering Laboratory of AIST, Japan is a prototype of the new mechanism that combines legs and wheels. Walk'n Roll has four legs, with a wheel attached at the end of each leg. The front legs have three joints, and a passive wheel is attached at the end of each. The rear legs have one joint and a relatively large active wheel attached at the end. The robot exhibits three locomotion modes: wheel mode, hybrid mode, and step mode. In the wheel mode, all the four wheels are used for locomotion. The leg motion can be used for steering. In the hybrid mode, the front two legs are used to walk. The step mode is used to climb or descend a large step. The rear wheel is moved from the rear side to the front side through the air by leg motion.

Another key factor is the inability to use one limb due to electromechanical failure. This would render the robot incapacitated. Limping is a biological phenomenon and would increase the performance of a quadruped in harsh and unstructured environments. The Birod program (Biomorphic Robot with Distributed Power) has been built at the University of Arizona (Ramohalli, 1999) to make space exploration more dependable.

The current paper presents our design for a quadruped with a frontal support/steering wheeled mechanism, followed by kinematics analysis, forward-pose-based gaits, and walking simulations.

II. SYSTEM DESCRIPTION

Figure 1 shows the arrangement of our quadruped with a support/steering wheel attachment. The robot consists of four identical legs (the right-side legs are symmetric to the left-side legs), each having two revolute joints (J1, J2) and one prismatic joint (J3). The first revolute joint swings the entire leg forward and aft at the body; the second revolute joint lifts the leg up and down (in a circle) at the shoulder; the prismatic joint lengthens and shortens the leg to meet the ground.

The support/steering wheels are on a steerable axle at the end of a fixed rod. This rod is attached to the body at the midpoint of its width. It is added to the Quadruped's body for added stability, allowing two legs to move at a time and still maintain static stability. Each leg has a 'claw' to increase stability of the system when any two legs are off the ground. The support/steering wheels would have the capability to rotate and maintain a commanded steering/h Heading angle. In conjunction with the legs, the steering angle controls the orientation of the robot. The support system can be modified to carry an appropriate tool and if suitably modified, could also work as a SCARA.

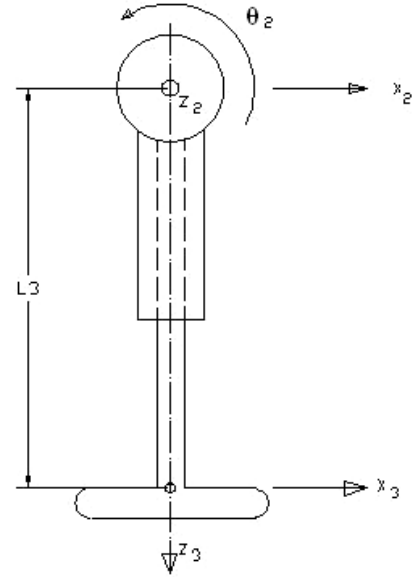


Figure 2. Kinematic Diagram of One (Right-Side) Leg

TABLE I
DH PARAMETERS FOR RIGHT-SIDE LEG

i	α_{i-1}	a_{i-1}	d_i	θ_i
1	0°	0	0	θ_{1j}
2	90°	0	L_2	θ_{2j}
3	90°	0	L_{3j}	0

The left-side leg DH parameters are the same as Table I, negating the second two α_{i-1} angles. The variables for each 3-dof leg are θ_{1j} , θ_{2j} , and L_{3j} . Note the index j indicates the four legs, $j = 1, 2, 3, 4$; L_2 is a fixed length shared by all four legs.

For calculating the center of gravity, we assumed masses for different sections of the robot. The body and legs were given a mass of 15; the shaft was given a mass of 3.5 and the steering system along with the wheels, 2.

III. POSE KINEMATICS MODELING

Pose kinematics relates the Cartesian position and orientation (pose) of each leg to the reference frame. Further, the pose of robot body center frame can be related to the Cartesian world the robot is walking in. Inverse pose kinematics is required for achieving general desired robot trajectories (i.e. placing each foot independently in 3D space). Forward pose kinematics is required for simulation and real-time sensor-based control.

In this paper, however, emphasis is given to the forward pose kinematics problem (i.e. calculate the XYZ coordinates of each foot and the support/steering wheels pose given the three leg joint variables for each of the four legs, plus the steering angle). Our current gaits are based on symmetric forward-pose motions. The inverse pose kinematics solution is given for completeness and future gait development.

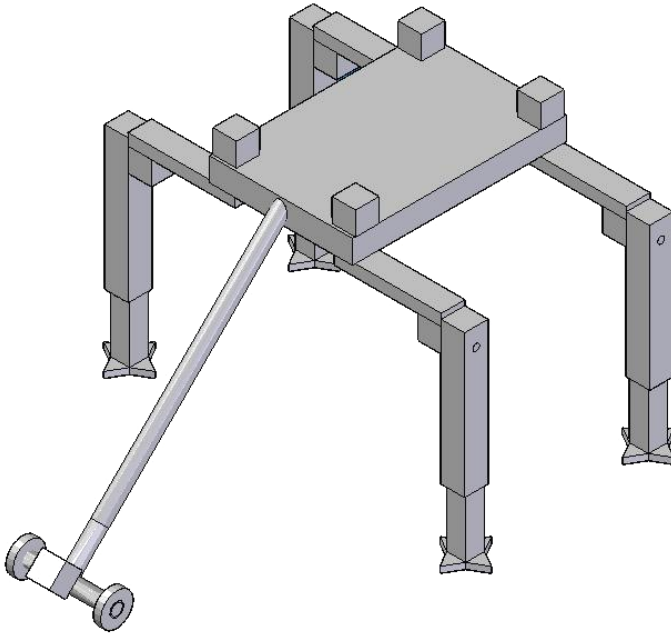


Figure 1. CAD model of Quadruped with Support/Steering Wheels

Figure 2 shows the kinematic model of one (right-side) leg. The Denavit-Hartenberg (DH, Craig (1989)) parameters for this leg are summarized in Table I below.

A. Forward Pose Kinematics

The forward pose kinematics (FPK) problem is stated: Given the eight active joint angles θ_{1j} and θ_{2j} , and the lengths of the four active prismatic joints L_{3j} ($j=1,2,3,4$), calculate the Cartesian pose of the each of the four robot legs, expressed by W_3T_j . This pose can then be interpreted and used for robot gait simulation. Note that first variable subscript is the joint index (1, 2, or 3) and $j=1,2,3,4$ is the leg index.

The schematic top view with frame assignments for Leg 1 is shown in Figure 3. We take the geometric center of the quadruped body as the moving reference $\{C\}$ frame. Initially, the $\{C\}$ frame coincides with the World frame $\{W\}$. All leg and support/steering wheels coordinate transformations are derived with respect to the moving $\{C\}$ frame. When the robot body changes position, we change the $\{C\}$ frame with respect to the $\{W\}$ frame with appropriate transformations.

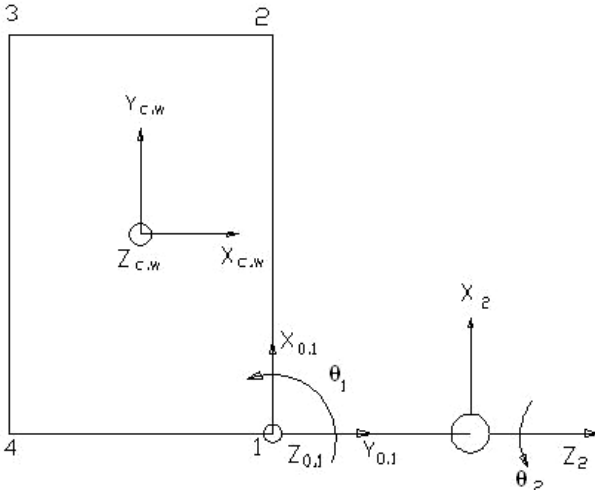


Figure 3. Schematic Top view of the robot showing the frame allocations.

The primary active homogeneous transformations for the right-side legs are shown in (1), giving the pose of the j^{th} foot with respect to the j^{th} $\{0\}$ frame at the body. Note that c and s are used to abbreviate *sine* and *cosine*, respectively.

$${}^0_3T_j = \begin{bmatrix} c\theta_{1j}c\theta_{2j} & s\theta_{1j} & c\theta_{1j}s\theta_{2j} & L_2s\theta_{1j} + L_{3j}c\theta_{1j}s\theta_{2j} \\ s\theta_{1j}c\theta_{2j} & -c\theta_{1j} & s\theta_{1j}s\theta_{2j} & -L_2c\theta_{1j} + L_{3j}s\theta_{1j}s\theta_{2j} \\ s\theta_{2j} & 0 & -c\theta_{2j} & -L_{3j}c\theta_{2j} \\ 0 & 0 & 0 & 1 \end{bmatrix} \quad (1)$$

The symmetric transformations for the left-side legs are in (2):

$${}^0_3T_j = \begin{bmatrix} c\theta_{1j}c\theta_{2j} & s\theta_{1j} & -c\theta_{1j}s\theta_{2j} & -L_2s\theta_{1j} - L_{3j}c\theta_{1j}s\theta_{2j} \\ s\theta_{1j}c\theta_{2j} & -c\theta_{1j} & -s\theta_{1j}s\theta_{2j} & L_2c\theta_{1j} - L_{3j}s\theta_{1j}s\theta_{2j} \\ -s\theta_{2j} & 0 & -c\theta_{2j} & -L_{3j}c\theta_{2j} \\ 0 & 0 & 0 & 1 \end{bmatrix} \quad (2)$$

The following transformation equation expresses the pose of the j^{th} foot with respect to the body center frame $\{C\}$ frame.

$${}^C_3T_j = {}^C_0T_j {}^0_3T_j \quad (3)$$

where C_0T_j are constant homogeneous transformation matrices giving the fixed pose of the j^{th} leg base frame $\{0\}$ with respect to the common $\{C\}$ frame. Now, the transformations relating the pose of each j^{th} foot frame with respect to the world frame $\{W\}$ are given below.

$${}^W_3T_j = {}^W_C T_j {}^C_3T_j \quad (4)$$

where ${}^W_C T_j$ is the transformation used to represent the pose of moving robot body reference $\{C\}$ with respect to the fixed $\{W\}$ frame. It initially is set to a 4 x 4 identity matrix and is modified correspondingly as the robot changes its position during walking.

The transformation matrix for the frame $\{S\}$ at the midpoint of the steering system to the $\{C\}$ frame is given by:

$${}^C_S T = \begin{bmatrix} 0 & -1 & 0 & 0 \\ 1 & 0 & 0 & E_y + 2 \\ 0 & 0 & 1 & -3 \\ 0 & 0 & 0 & 1 \end{bmatrix} \quad (5)$$

where E_y is the distance along the Y-axis from the $\{C\}$ frame to the point where the steering shaft begins. When the steering wheel is set to an angle ϕ , the transformation matrix ${}^W_C T$ is modified to

$${}^W_C T = \begin{bmatrix} c\phi & -s\phi & 0 & -\delta \cdot s\phi \\ s\phi & c\phi & 0 & \delta \cdot c\phi \\ 0 & 0 & 0 & 0 \\ 0 & 0 & 0 & 1 \end{bmatrix} \quad (6)$$

where δ is the incremental displacement (= 0.6 for this simulation) in the forward direction.

B. Inverse Pose Kinematics

The inverse pose kinematics problem for one leg is stated: Given the desired foot pose 0_3T_j , calculate the three active j^{th} leg joint variables θ_{1j} , θ_{2j} , and L_{3j} . We extract the Cartesian coordinates of the position vector from the given transformation matrix 0_3T_j as $\{x \ y \ z\}^T$. We obtain coupled transcendental equations, the solutions of which are given below for one of the right-side legs.

$$\begin{aligned} \theta_{1j} &= 2 \tan^{-1} \left[\frac{x \pm \sqrt{y^2 + x^2 - L_2^2}}{L_2 - y} \right] \\ \theta_{2j} &= a \tan 2 \left(\frac{x - L_2 \sin \theta_{1j}}{\cos \theta_{1j}}, -z \right) \\ L_{3j} &= \frac{z}{-\cos \theta_{2j}} \end{aligned} \quad (7)$$

There are two solutions for θ_{lj} and one solution θ_{2j} and L_{3j} for each; therefore, there are two overall IPK solution sets for each leg.

The IPK solution for the left side legs will be similar: The symmetry of the robot allows us to use the same angles with opposite signs for the left side legs.

In the current paper we use FPK simulation to construct our gaits, enforcing symmetry on diagonally opposite legs. Hence, the inverse pose kinematics has not yet been used in our gaits. We will extend our gaits to more general IPK-based methods in the future. Thus, we will focus more on the multiple solutions and singularities in future work. For simplicity, we have omitted the wheels in the simulation. We assume, without loss of generality, that the center of mass of the wheel system lies at the midpoint of the line joining the centers of the wheels.

IV. GAIT DESIGN

The gait employed for this robot resembles a reptilian trot. Due to the inherent static stability of our system (thanks to the support/steering wheels), two legs can be lifted off the ground at any time, during normal gait. Diagonally opposite legs are linked together symmetrically to simulate a virtual biped gait. The joint variable commanded to the three joints is the same for both legs. Like a human bipedal gait, the robot ‘falls forward’ (via pushing from the two grounded legs) after the first pair is off the ground. The presence of the support/steering wheels prevents the robot from toppling over.

A. Walking in a Straight-Line Path

This section presents the sequence of events leading to straight-line forward motion of the robot, as demonstrated in the simulation of Figures 3. First, legs 1 and 3 are lifted off the ground (see Figure 4b). They are then moved to their maximum joint limits on both revolute joints on each leg. Then the prismatic joint L_{3j} is extended to reach the ground. At this point of time, two events happen in parallel. Legs 1 and 3 straighten themselves, using the frictional force to push the body frame forward. At the same time, legs 2 and 4 lift off the ground. This entire cycle repeats again with legs 2 and 4. This drives the body forward as demonstrated in the series of diagrams. The steering heading angle is maintained at nominal (zero angle) so the passive wheels are rolling straight ahead.

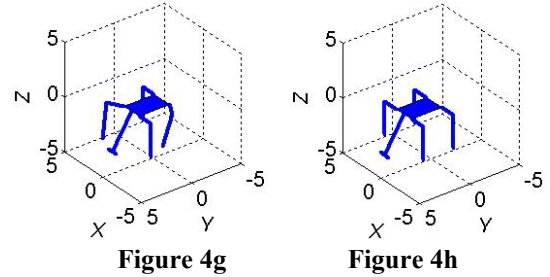
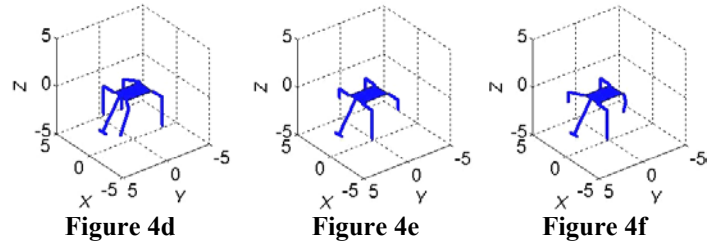
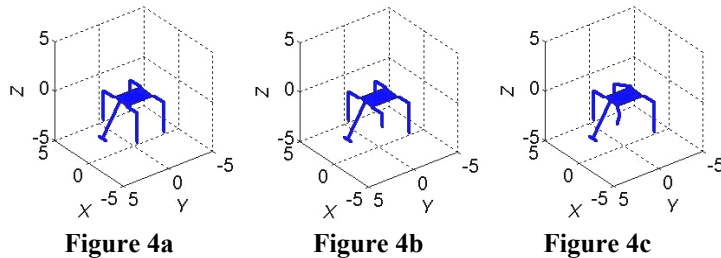


Figure 4. Gait Simulations for Straight-Line Trajectory

The center of gravity of the system is plotted at each instant to verify that static stability constraints are satisfied. Snapshots of the static stability polygons for positions 4b, 4c and 4d are shown in Figures 5.

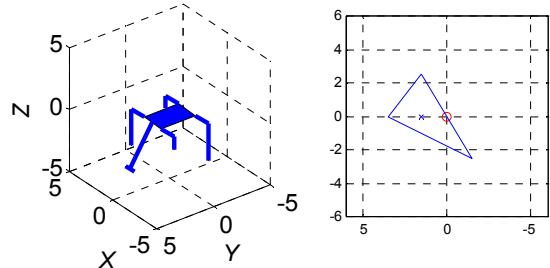


Figure 5a. Static Stability Polygon for Figure 4b

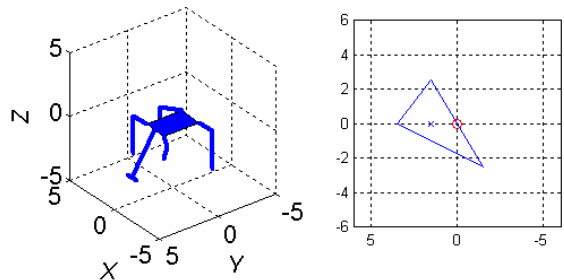


Figure 5b. Static Stability Polygon for Figure 4c

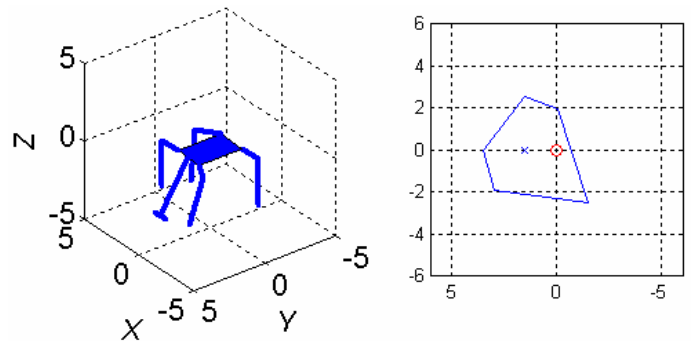


Figure 5c. Static Stability Polygon for Figure 4d

Figure 5. Plots showing the Center of gravity of the system

The ‘O’ mark on the diagrams in Figures 5 is the center of gravity of just the quadruped with legs but without the support/steering wheel. The ‘X’ mark on the diagrams is the center of gravity of the entire system. It can be seen that the center of gravity of the entire system doesn’t is close to the quadruped’s center of gravity; this is true for all motions.

B. Walking along a Curved Path

When the steering wheel is controlled to desired angles, the robot walks along a curved path. The legs power the body forward and the steering mechanism sets the trajectory. Intuitively, the body will follow where the steering mechanism goes. If the steering angle is constant and non-zero, the curve will be a circle. The appropriate ${}^W_C T$ transformation gives the next set of Cartesian coordinates and also the orientation of the robot. In our simulation, we set the robot on an infinite loop to move by 10 degrees to the left every step (tracing a circle). Two snapshots of the robot at different positions along the trajectory are shown in Figures 6 below.

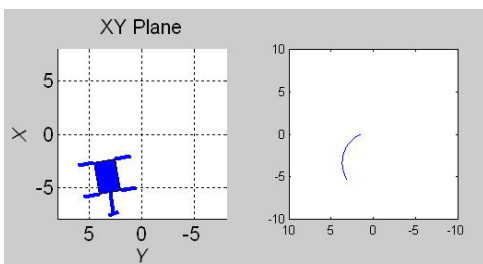


Figure 6a

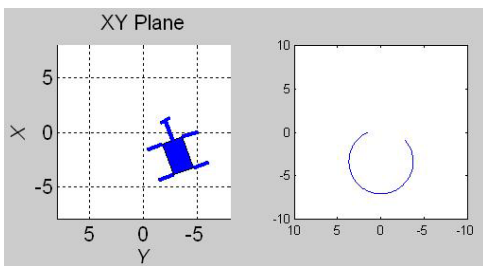


Figure 6b

Figure 6. Gait Simulations for a Curvilinear Trajectory

C. Limping in the Case of Failure

This is a unique feature that our preliminary investigation has given us. We have designed the robot so that when one of the legs was disabled and the gait correspondingly modified, the robot could still carry on forward motion. This is a first step (pun intended!) towards one-failure-safe operation.

We simulated Leg 3 to be handicapped. We then modified the gait in the following fashion: Leg 1 lifts up, balancing the body on Leg 2, Leg 4 and the support wheel. Then Leg 2 moves forward, comes down and advances the body frame forward. This

is shown in Figures 7 (a)-(c). Leg 2 repeats the same. This is shown in Figures 7 (d)-(e). It is obvious that this particular sequence is unique to the failure of Leg 3. Hence, the on-board processor has to correctly determine which leg is at fault and run the corresponding limping routine. This adds a design constraint in that each leg should be powerful enough to drag the entire body frame forward.

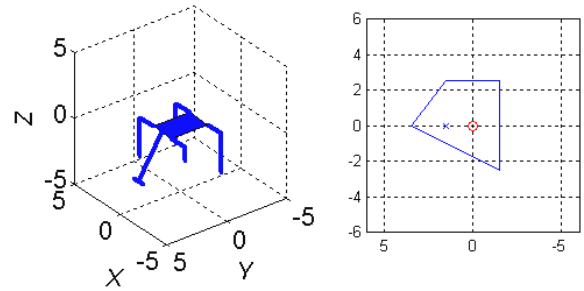


Figure 7a

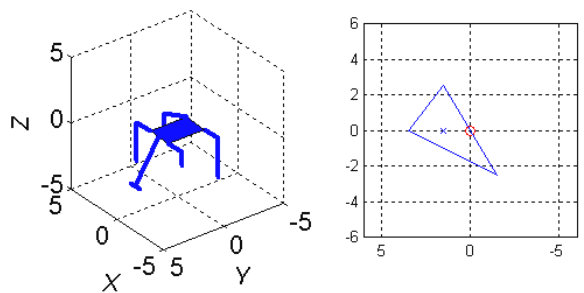


Figure 7b

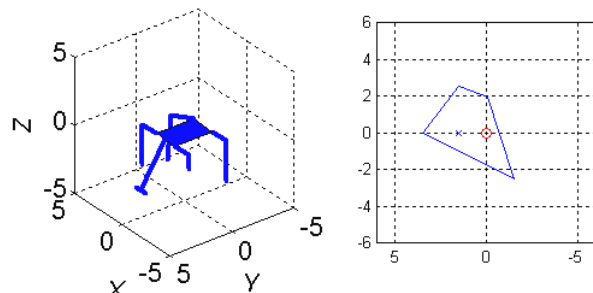


Figure 7c

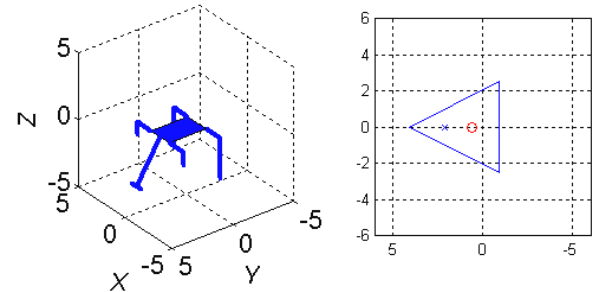


Figure 7d

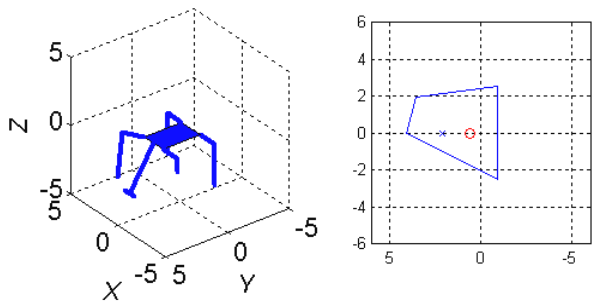


Figure 7e

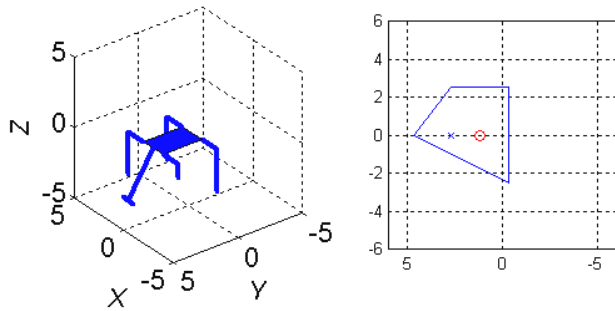


Figure 7f

Figure 7. Gait during Limping

V. CONCLUSION

This paper presents a new design solution addressing static stability issues for a walking quadruped robot. We presented our concept, followed by forward and inverse pose kinematics. We then presented examples for linear, curvilinear and limping gaits and observed the position of the center of mass at every instance (it must remain within the grounded foot polygons to ensure static stability). To date we have used simple, symmetric FPK-based gaits. We will develop general IPK-based gait methods to complement this simple approach. IPK-based methods will be developed at two levels: 1. at the leg level, to allow general placement of each foot relative to the body; and 2. at the world level, i.e. controlling the walking of the robot in the global Cartesian frame. Thus far we have focused on planar motions but we will soon consider general 3D walking motions and gaits.

The results obtained were encouraging and we plan to build a model of the system. We are working on commanding the robot to follow complicated curves. Due to the relatively small hardware requirements on board, we plan to incorporate a simple arm to enable pick and place operations. We ultimately plan to

make an amphibious biomimetic robot capable of traversing hostile terrain.

REFERENCES

- Boone, Gary, and Hodgins, Jessica. "Walking and Running Machines". *The MIT Encyclopedia of the Cognitive Sciences*, MIT Press, 1998
- Bucket, J. R. (1977). *Design of an On-board Electronic Joint System for a Hexapod Vehicle*. Master's thesis, Ohio State University
- Craig, J.J (1989), "Introduction to Robotics: Mechanics and Control", *Addison Wesley Publishing Co., Reading, MA*.
- Hirose, S., and Y. Umetani. (1980), "The basic motion regulation system for a quadruped walking machine.", *American Society of Mechanical Engineers Paper 80-DET-34*.
- Hirose, Shiego, Kato, Keisuke Source (2000), "Study on Quadruped walking robot in Tokyo Institute of Technology – past, present and future". *IEEE International Conference on Robotics and Automation, v1 2000, p414-419*.
- McGhee, R. B. (1983), "Vehicular legged locomotion." In G. N. Saridis, Ed., *Advances in Automation and Robotics*. JAI Press.
- Quinn, R. D. Nelson, G.M., Bachmann, R.J., Kingsley, D.A., Offi, J. and Ritzmann, R. E. (2001). "Insect Designs for Improved Robot Mobility." *In Proc. of Climbing and Walking Robots Conference (CLAWAR01), Professional Engineering Publications*, edited by Berns and Dillmann, Karlsruhe, Germany, pp. 69-76.
- Simmons, R., E. Krotkov, W. Whittaker, and B. Albrecht. (1992). "Progress towards robotic exploration of extreme terrain.", *Applied Intelligence: The International Journal of Artificial Intelligence, Neural Networks and Complex Problem-Solving Technologies* 2(2): 162–180.
- Song, S. M., and K. J. Waldron. (1989). "Machines That Walk." Cambridge, MA: MIT Press.

<http://vpr2.admin.arizona.edu/ror/Volume16-1/birods.htm>

<http://www.aist.go.jp/MEL/mainlab/rob/rob08e.html>